European Review for Medical and Pharmacological Sciences 2024; 28: 584-602

A comprehensive analysis of essential meiotic endonuclease 1 to prognosis and immune infiltration in kidney renal clear cell carcinoma

H.-D. LI[1], H.-X. MA[2], J.-H. MA[3], S.-P. KONG[1], S.-T. ZHAO[1], S.-Q. FAN[1], F. QIN[1], J.-G. MA[1]

[1]Department of Urology, The Third Hospital of Hebei Medical University, Shijiazhuang, China
[2]Faculty of Health and Behavioural Sciences, The University of Queensland, Queensland, Australia
[3]Geriatrics Department, Hebei Chengde Central Hospital, Chengde, China

H.-D. Li and H.-X. Ma contributed equally to this work

Abstract. – OBJECTIVE: **Clear cell renal cell carcinoma (ccRCC) is the most common type of cancer, and its molecular pathogenesis is unclear. In this study, we investigated the prognostic value of essential meiotic endonuclease 1 (*EME1*) in kidney renal clear cell carcinoma (KIRC).**

MATERIALS AND METHODS: **We downloaded the RNA-Seq expression of 526 KIRC tissues and 72 normal tissues from the TCGA database and the corresponding clinical data. The gene expression profiles associated with four clear cell renal cell carcinomas were downloaded from the GEO database for analysis. The expression of *EME1* in clear renal cell carcinoma and its correlation with the clinical baseline data were analyzed. Kaplan-Meier survival curve analysis was performed to assess the relationship between *EME1* and patient survival. Enrichment analysis was performed to elucidate the possible functions of *EME1*. We also analyzed the relationship between the *EME1* expression and immune infiltration through TIMER2.0 and TISIDB online databases as well as the relationship between *EME1* and common immune checkpoints.**

RESULTS: ***EME1* was identified as a risk factor for overall survival in clear cell renal cell carcinoma with a hazard ratio of 3.201 (95% confidence interval: 2.430-4.215; $p < 0.001$). *EME1* was highly expressed in KIRC compared to that in normal tissues ($p < 0.001$) and in the worse TNM stages and late stages (stage 3/4) ($p < 0.001$). High *EME1* expression was strongly associated with the advanced T stage ($p = 0.003$), advanced N stage ($p = 0.002$), and advanced M stage ($p = 0.006$). Research data on KIRC were simultaneously collected and analyzed from the GEO database, including GSE40435, GSE53000, GSE68417, and GSE53757. *EME1* predicted the survival status in KIRC patients (AUC = 0.62). We further established a nomogram including the correlation between the high and low *EME1* expression, and *EME1* was found to contribute to the prediction of the probability of patient survival with a c-index = 0.796. Kaplan-Meier analysis revealed a lower likelihood of survival with a high *EME1* expression ($p < 0.001$). In addition, further bioinformatics analysis suggested that EME1 may be associated with the extent of immune infiltration in KIRC.**

CONCLUSIONS: **An increased expression of EME1 in KIRC is thus associated with advanced clinicopathological features, possibly acting as a potential biomarker of poor prognosis in KIRC.**

Key Words:
EME1, Clear cell renal cell carcinoma, Prognosis, Immune infiltration.

Introduction

The incidence of renal cell carcinoma (RCC) has increased recently, with 76,080 cases of kidney and renal pelvis cancer diagnosed only in the USA in 2021, claiming the lives of 13,780 people[1]. There are several subtypes of RCC, and approximately 70% of individuals are diagnosed with clear cell RCC (ccRCC). Of these, up to one-third of cases develop or progress to metastasis[2], and metastatic RCC (mRCC) poses a significant medical burden[3]. RCC cells may induce cytokine expression in the tumor microenvironment (TME) during tumorigenesis and growth phases, leading to the development of an immunosuppressed tumor state and the promotion of immune escape[4]. RCC is considered an immunogenic tumor that mediates immune dysfunction largely by induc-

Corresponding Author: Jianguo Ma, MD; e-mail: mjg197103@163.com

ing infiltration of immunosuppressive cells (e.g., regulatory T cells [Tregs] and bone marrow-derived suppressor cells) into the TME[5]. Thus, there is a need to find new prognostic biomarkers that can accurately predict patient survival as well as provide new ideas for determining new targeted therapies for subsequent ccRCC.

Initially, essential meiotic endonuclease 1 (*EME1*) was detected in *Schizosaccharomyces pombe*, showing interaction with methyl methanesulfonate-sensitive UV-sensitive 81 (Mus81), which itself has no endonuclease activity and must interact with Mus81 to exert an endonuclease activity[6]. Subsequently, related experiments in mice revealed that *EME1* deficiency led to spontaneous genomic instability, where mammalian *EME1* played a key role in DNA repair and the maintenance of genomic integrity[7]. Chromosomal instability (CIN) has been associated with cancer evolution, with possible relevance to drug resistance and poor prognosis, and the constitution-specific nucleic acid endonuclease *Mus81-Eme1* has been reported to prevent CIN, while aberrant processing of late replication intermediates by *Mus81-Eme1* has been identified as the source of CIN[8]. Another study[9] revealed that tumors with low *EME1* expression were more sensitive to antitumor drugs than those with high *EME1* expression. Identification of *EME1* as a cisplatin resistance marker is expected to facilitate the development of resistance modifiers or new molecularly targeted drugs[10]. Similarly, cetuximab promotes *EME1* stability and elevates the *EME1* protein levels, which in turn promotes DNA repair in tumor cells, resulting in the development of drug resistance[11]; thus, colorectal cancer cells lacking both DNA damage repair protein *EME1* and *MUS81* are more sensitive to chemotherapeutic drugs[12]. This line of thought signifies a correlation between the overexpression of *EME1* and the development of resistance to late chemotherapy in tumors.

Some scholars[13] have revealed an association between *EME1* and the recurrence of bladder cancer after surgery. Elevated levels of *EME1* in gastric cancer (GC) indicate poor prognosis in patients, and it has been identified that *EME1* can activate the Akt/GSK3B/CCND1 pathway to make GC more invasive and inhibit apoptosis, which contributes to the poor prognosis of GC patients[14]. Exon mutants of *EME1* can significantly increase the risk of early-onset breast cancer in women[15]. In addition, elevated *EME1* was found to be associated with reduced overall survival (OS) in patients with esophageal cancer, with increased sensitivity to oxaliplatin treatment when the *EME1* expression was lacking in cancer cells[16]. This finding suggests that *EME1* is associated with cancer development as well as poor prognosis and treatment resistance, possibly acting as a biomarker for tumors. However, the regulatory relationship of *EME1* in the development of clear cell renal cell carcinoma remains unclear.

Considering this situation, we analyzed the relevant data of kidney renal clear cell carcinoma (KIRC) in TCGA and GEO databases to assess the potential correlation between *EME1* expression in the KIRC tissues as well as the clinicopathological information of these patients. In addition, we assessed whether *EME1* expression can act as an independent prognostic biomarker for OS in ccRCC patients. Accordingly, the correlation between *EME1* and tumor-infiltrating immune cells was further analyzed. Finally, some genes associated with *EME1* and their prognosis in KIRC were analyzed. Thereby, bioinformatics was applied to explore the possible potential relevance of *EME1* for the development of ccRCC and the related mechanisms.

Materials and Methods

Data Source and Analysis

We downloaded KIRC cancer-associated RNA sequences, clinicopathology, and survival data on the UCSC Xena network (https://xenabrowser.net/datapages/), We employed the R package DESeq2 and used | logFC |>1 and p_{adj}<0.05 as thresholds to further select differential analysis of mRNA expression in the normal and tumor groups so as to obtain differentially expressed genes (DEGs); the "ggpubr" and "ggthemes" R packages for volcano plotting and the "survival" and "forestplot" R package were used to draw forest plots to represent the hazard ratio of different genes. The top 10 genes were selected in accordance with their ranking of the *p*-value from the smallest to the largest. We further obtained four gene expression profiles on KIRC from the GEO database (https://www.ncbi.nlm.nih.gov/geo/), including GSE40435, GSE53000, GSE68417, and GSE53757. The GSE40435 dataset was obtained by using the GPL10558 platform and it included 101 adjacent normal kidney tissues and 101 KIRC tissues. The GSE53000 dataset was obtained using the GPL6244 platform and included

6 normal kidney tissues and 56 KIRC tissues. The GSE68417 dataset was obtained using the GPL6244 platform and included 14 normal kidney tissues and 29 KIRC tissues. The GSE53757 dataset was obtained using the GPL570 platform and included 72 normal kidney tissues and 72 KIRC tissues. This information was collected from the GEO database and analyzed using the "limma" R package. The abovementioned data were used to analyze the expression of *EME1* in the KIRC tissues, and the difference in the expression of *EME1* between the tumor and normal tissues was demonstrated with dot plots.

Creation of the Nomogram about KIRC

Based on the clinicopathological and survival data of KIRC downloaded from the UCSC Xena network, the patient age, gender, race, and TNM stage were selected as data for analysis, while the missing values were removed and the *EME1* expression was added (the cutoff value of *EME1* expression was determined by the median value) to determine the predictive level of survival of the KIRC patients. The predictive accuracy of the model was assessed by using C-index.

Clinicopathological Features of EME1 Expression in KIRC

The high and low *EME1* expression groups were assessed based on the median *EME1* expression, and the patient's age, gender, race, and TNM stage were selected as data for analysis. The missing values were removed for subsequent analysis of the impact of *EME1* expression differences on the clinicopathological profile of KIRC patients.

Survival Prediction of EME1 for KIRC

We extracted the survival information of each sample in TCGA. The receiver operating characteristic (ROC) curve and Time-Dependent ROC Curve (timeROC) were used to evaluate the feasibility of using *EME1* as a differentiating factor by the area under the curve (AUC) score. We used the "ROC", "rms", and "timeROC" R packages to plot the analysis results.

EME1 Expression Affects Patient Survival

We extracted the survival information from each sample in TCGA, which included the survival status and survival time, and divided the patients into high and low expression groups based on the median value of the *EME1* expression as the cut-off point, analyzed the difference in the survival probability among patients with different *EME1* expression, and plotted the Kaplan-Meier curve of the survival rate by using the "survival" R package.

Functional Prediction and Mechanism Investigation

Enrichment analysis was performed to compare the low and high *EME1* expression datasets as well as to identify the different signaling pathways in KIRC and the associated biological functions. A preliminary list of gene classifications was generated based on the correlation of these DEGs with the *EME1* expression. Significant differences were observed between the high and low *EME1* groups. Based on the gene classification list, we performed GO, KEGG, and GSEA enrichment analyses with the "org.Hs.eg.db" and "clusterProfiler" R packages for analysis and mapping.

Immune Infiltration in KIRC and Infiltration of Immune Cells with DEGs

We analyzed the infiltration of different immune cells in different patient tissues based on the expression profiles of KIRC patients with the "e1071", "parallel", and "preprocessCore" R packages to analyze and plot the results. We also analyzed the differences in the infiltration levels of immune cells in KIRC in 22 different genes based on 10 DEGs. The "corrplot" R package was applied to plot the images. TIMER2.0 (http://timer.cistrome.org/) database was applied to determine the immune cells with relevance to KIRC tissues based on the *EME1* expression data and their tumor purity and infiltration, including CD8, Mast, Tfh, and Trg infiltration as well as the corresponding survival differences.

TISIDB

We used TISIDB, a comprehensive repository portal for tumor-immune system interactions, to analyze the relationship between the *EME1* expression and different human cancers, as well as the relationship between the *EME1* expression and differences in immune checkpoints among clear cell renal cell carcinomas and OS.

Pan-Cancer Analysis and the Associated Survival Analysis by GEPIA

GEPIA (http://gepia.cancer-pku.cn/) was used as a tool to conclude pan-cancer. We employed this database to further analyze the differential expression of *EME1* in different tumors.

LinkedOmics Database Analysis

We used the LinkedOmics database (http://www.linkedomics.org/login.php) for the statistical analysis of genes associated with *EME1*. Volcano and heat maps were employed to represent the associated genes. Scatter plots were used to represent the top 5 genes that were positively or negatively associated with *EME1*. For the genes associated with *EME1*, we further analyzed the relationship between their expression and KIRC survival by using the GEPIA database.

Statistical Analysis

The differences in the *EME1* expression between the normal and tumor tissues were compared by the Wilcoxon rank-sum test, and the correlation between the *EME1* expression and clinical and pathological parameters was tested by Chi-square test using the SPSS software version 20. Differences in the OS between the high and low expression groups were compared with the Kaplan-Meier curves, and the *p*-values were calculated by log-rank test. The survival package in R software was used for the abovementioned tests. The relationship between the *EME1* expression and the related gene expression in KIRC was analyzed by using Pearson's correlation test. $p < 0.05$ was considered to indicate statistical significance. SPSS 20.0 (IBM Corp., Armonk, NY, USA) and R software (version 4.0.5) was employed for statistical analysis.

Results

Expression of EME1 in KIRC and Prognostic Correlation with KIRC

We retrieved cancer-associated mRNAs from KIRC by searching the cancer gene atlas and downloading them from the UCSC Xena network, which we analyzed by R software (version 4.0.5) (5891 abnormally expressed mRNAs, including 3800 upregulated and 2091 downregulated mRNAs; the fold change was ≥1, $p < 0.05$), and plotted volcanoes (Figure 1A). Next, the hazard ratio forest plot was drawn by evaluating the effect of differential gene expression on patient survival, and the top 10 genes, including the *EME1* gene, were ranked by the *p*-value from the smallest to the largest (Figure 1B).

To assess the difference in the *EME1* expression between the tumor and normal tissues, we analyzed the mRNA sequencing data obtained from TCGA (including 526 KIRC and 72 normal samples) using the R software. The results revealed that *EME1* was overexpressed in the KIRC tumor tissues relative to that in the normal tissues ($p < 0.001$) (Figure 1C). We further analyzed the expression of *EME1* at different TNM stages of KIRC patients and found that patients with higher TNM stages showed higher *EME1* expression in the tumor tissues ($p < 0.001$) (Figures 1D-F). Accordingly, we analyzed the difference in the *EME1* expression in KIRC patients with tumors at different stages and found that tumors with more advanced stages (stages 3/4) had a significantly high expression of EME1 ($p<0.001$) (Figure 1G). In summary, our results showed that *EME1* was highly expressed in the KIRC tissues, and it was associated with poorer staging and grading of clear cell renal cell carcinoma. We further validated these findings by collecting data from the four GEO datasets and analyzing them, which showed that *EME1* was highly expressed in KIRC (Figures 1H-K). GSE40435 (Figure 1H, $p < 0.001$), GSE53000 (Figure 1I, $p < 0.001$), GSE68417 (Figure 1J, $p < 0.001$), and GSE53757 (Figure 1K, $p < 0.05$).

After collecting the survival status and survival time of KIRC patients, we first considered the important role of *EME1* overexpression in the prognosis prediction of KIRC. We performed ROC curve analysis as well as time-dependent ROC analysis to evaluate the predictive ability of *EME1* in KIRC patients (Figures 1L and M). We found that the AUC for both analyses was > 0.60, which implied a good accuracy of *EME1* in predicting the survival time of KIRC patients.

The Kaplan-Meier analysis was performed to examine the prognostic value of EME1 expression in KIRC patients, dividing them into high and low groups based on the cutoff value (the median expression of *EME1*). We noted a significantly longer survival time in the *EME1* low expression group than in the high expression group, and a greater number of patients in the *EME1* low expression group were present in the longer survival time phase ($p < 0.001$ Figure 1N). Overall, we detected a significant negative correlation between the expression of *EME1* and the survival rate of KIRC patients.

EME1 Expression Was Correlated with Clinicopathological Features of KIRC

Table I depicts some necessary clinical information on 247 KIRC patients, including their age, gender, race, and TNM stage. We determined a

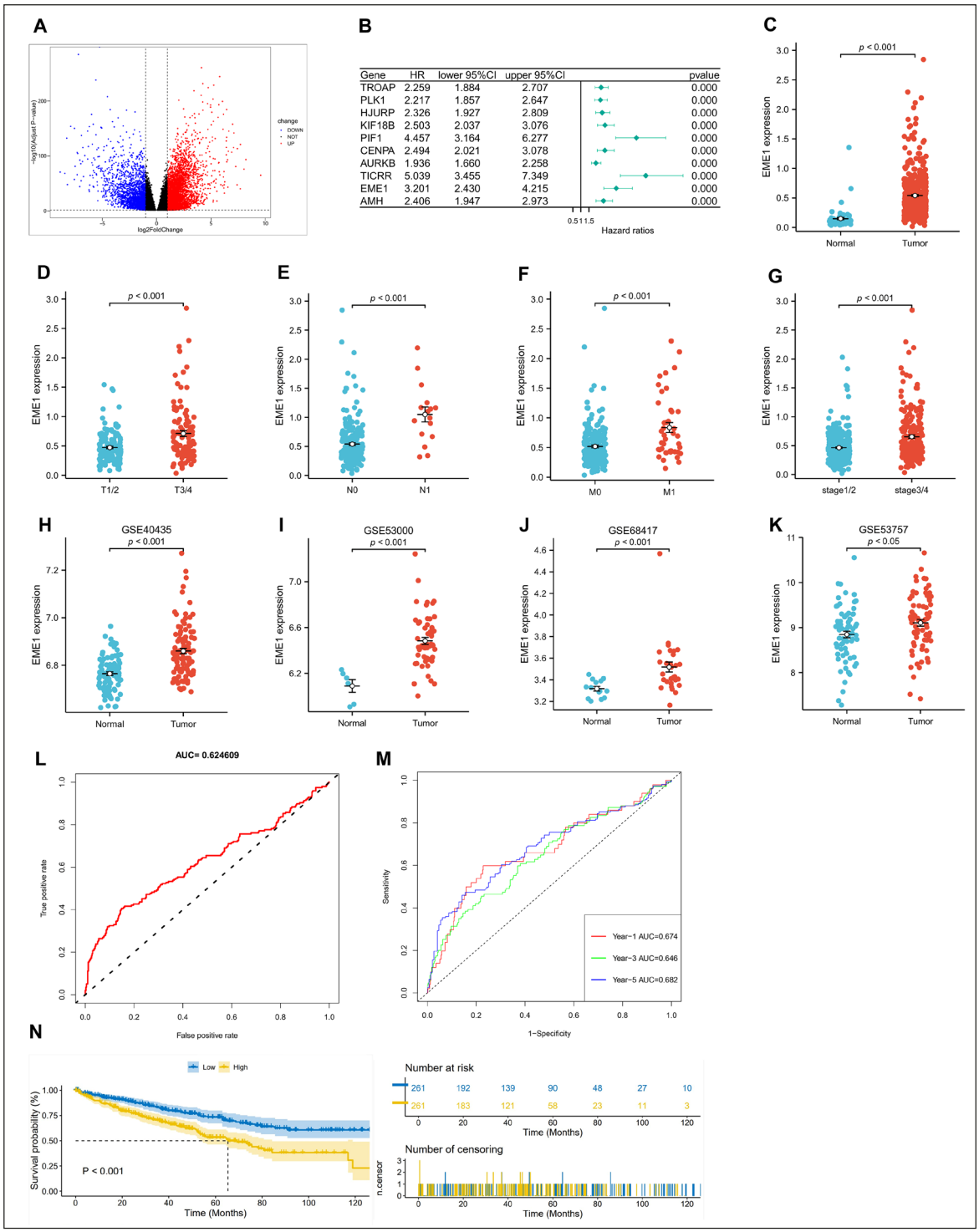

Figure 1. Differential expression of *EME1* in KIRC. **A**, The volcano plot analysis of clear cell renal cell carcinoma and normal tissues in the TCGA database. **B**, Univariate Cox regression analysis of differential genes. (The top 10 genes are sorted according to the *p*-value). **C**, Differential expression of *EME1* in different disease states (tumor or normal). **D-F**, Differences in the *EME1* expression at different TNM stages. (Owing to the missing values, a total of 247 patients were involved in the analysis of the *EME1* expression at different TNM staging). **G**, Differential expression of *EME1* in different cancer stages. (Based on the information of 320 stage1/2 patients and 204 stage3/4 patients in the TCGA database). **H**, The expression of *EME1* in the GSE40435 dataset. **I**, The expression of *EME1* in the GSE53000 dataset. **J**, The expression of *EME1* in the GSE68417 dataset. **K**, The expression of *EME1* in the GSE53757 dataset. **L**, In the ROC, the area under the curve (AUC) reached 62.4%. **M**, In the time-dependent ROC, the AUC of 1,3, and 5 years reached 67.4%, 64.6%, and 68.2%, respectively. **N,** The survival curves of *EME1* differential expression by Kaplan-Meier analysis.

Table I. Clinicopathological features of *EME1* expression in 247 clear cell renal cell carcinoma tissue samples.

Group	Number	EME1 expression		χ^2	*p*-value
		High, n [%]	Low, n [%]		
Age				0.688	0.407
≤ 50	49	27 [55]	22 [45]		
> 50	198	96 [49]	102 [51]		
Gender				0.360	0.548
Female	97	46 [47]	51 [53]		
Male	150	77 [51]	73 [49]		
Race				3.664[a]	0.194
Asian	4	1 [25]	3 [75]		
White	229	118 [52]	111 [48]		
Black or African American	14	4 [29]	10 [71]		
T stage				9.132	0.003*
T1 and T2	144	60 [42]	84 [58]		
T3 and T4	103	63 [61]	40 [39]		
N stage				9.728	0.002*
N0	231	122 [53]	109 [47]		
N1	16	14 [88]	2 [12]		
M stage				7.501	0.006*
M0	205	94 [46]	111 [54]		
M1	42	29 [69]	13 [31]		

[a]Fisher's Exact Test. *$p < 0.05$ indicates statistical significance.

correlation between the *EME1* expression and clinicopathological features of KIRC. A high expression of *EME1* correlated with advanced T stage ($\chi^2 = 9.132$, $p = 0.003$), advanced N stage ($\chi^2 = 9.728$, $p = 0.002$), advanced M stage ($\chi^2 = 7.501$, $p = 0.006$) were correlated. However, there was no statistically significant association between the *EME1* expression and patients' age, gender, and race.

We established a nomogram based on various clinical data of patients (including age, gender, race, TNM stage, and the risk and *EME1* expression), where the *EME1* expression was distinguished from high and low expression by the median value. This value was then used to determine the survival rates of KIRC patients at 1, 3, and 5 years (Figure 2). Considering the scale of each point, we intuitively concluded that the high expression of *EME1* contributes to the judgment of prognosis. This model was judged to have a c-index of 0.796 and a corrected-c-index of 0.769 (nomogram model for predicting 1-year, 2-year, and 3-year OS in KIRC patients). When using the column line graph, all points identified on the scale for each variable were summed. The total number of points predicted on the bottom scale indicates the probability of 1-year, 2-year, and 3-year survival.

Enrichment Analyses in EME1 Expression Phenotype

To explore *EME1*-mediated molecular functions at KIRC, DEGs were selected between the high and low *EME1* expression datasets and shown to be enriched to pathways with significant differences. Based on the results of KEGG analysis, the pathways involved mainly included neuroactive ligand-receptor, calcium signaling pathway, RAS signaling pathway, pancreatic secretion, and serotonergic synapse (Figure 3A). From the GO analysis results, we learned that the gene functions involved mainly included the meiotic cell cycle process, cell fate commitment, meiotic cell cycle, mitotic nuclear division, humoral immune response, and nuclear division organelle fission (Figure 3A). In addition, we conducted GSEA analysis and found that a high expression of *EME1* was associated with biological functions such as cell cycle G2 M phase transition, mitotic cell cycle, post-transcriptional regulation of gene expression, and the regulation of cell cycle G2 M phase transition (Figure 3B). These results indicated that *EME1* may play a potential role in cancer cells by affecting the cell cycle and cell division. Thus, *EME1* may serve as a potential prognostic marker of prognosis and therapeutic target in KIRC.

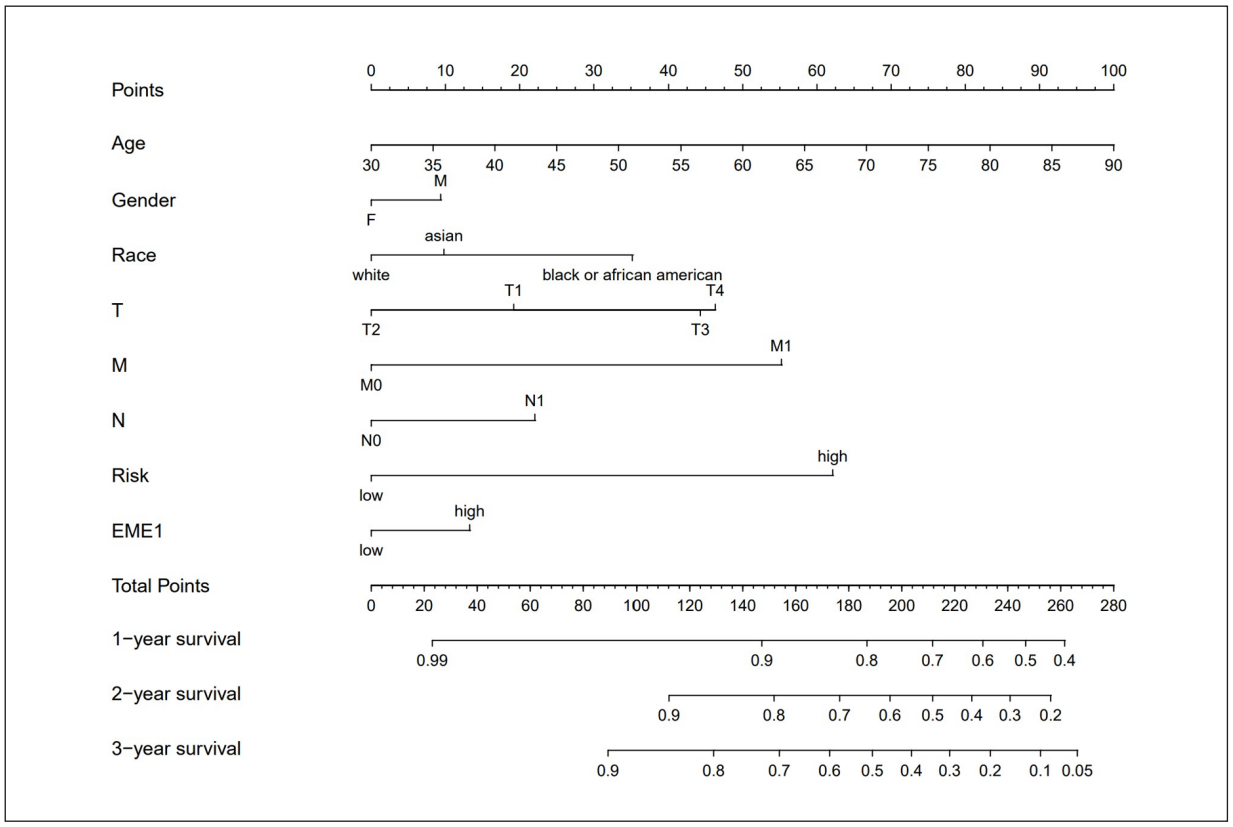

Figure 2. Nomogram model predicting the 1, 2, and 3-year OS in patients with clear cell renal cell carcinoma. The nomogram was employed by summing all points identified on the scale for each variable. The total points projected on the bottom scales indicate the probabilities of 1, 2, and 3-year survival.

Relationship Between EME1 Expression and Immune Cell Infiltration

First, we assessed the immune cell infiltration status in the tumor tissues of KIRC patients and the alterations in the 10 genes of the immune cells in tumor tissues by using the CIBERSORT algorithm (Figures 4A and B). We initially found a correlation between *EME1* and follicular helper T cells, Tregs, mast cells, and CD8+ T cells. Subsequently, we employed TIMER2.0 to analyze the correlation between the *EME1* expression and the level of immune infiltration in KIRC as well as the cumulative survival of KIRC. Our results indicated that the expression of *EME1* was positively correlated with the infiltration level of CD8+ T cells (r = 0.174, p = 1.73e-04), follicular helper T cells (r = 0.287, p = 3.24e-10), and Tregs (r = 0.222, p = 1.55e-06) and negatively correlated with the infiltration level of mast cells (r = -0.135, p = 3.76e-03) (Figure 5A). In addition, we noted that the cumulative survival in clear cell renal cell carcinoma was associated with follicular helper T cells, Tregs, and mast cells. Among these, a low level of mast cell infiltration was associated with a poor cumulative survival rate, and the expression of *EME1* was negatively correlated with mast cells as indicated above. It is also known that mast cell infiltration may be associated with a better prognosis in clear cell renal cell carcinoma, whereas the *EME1* expression decreased the number of mast cells. It is conjectured that this cause may be one of the reasons for the poorer prognosis of KIRC due to high *EME1* expression. These analyses cumulatively suggest that *EME1* is involved in the immune infiltration of KIRC (Figure 5B).

For these results, we further analyzed whether there is a function of *EME1* in KIRC that allows tumor cells to undergo immune escape. The TISIDB results suggested that a high expression of *EME1* in clear cell renal cell carcinoma was correlated with a high expression of a series of immune checkpoints (Figure 5C), which mainly included PDCD1, LAG3, CTLA4, and LGALS9 (Figures 5D-G). In summary, *EME1* may pro-

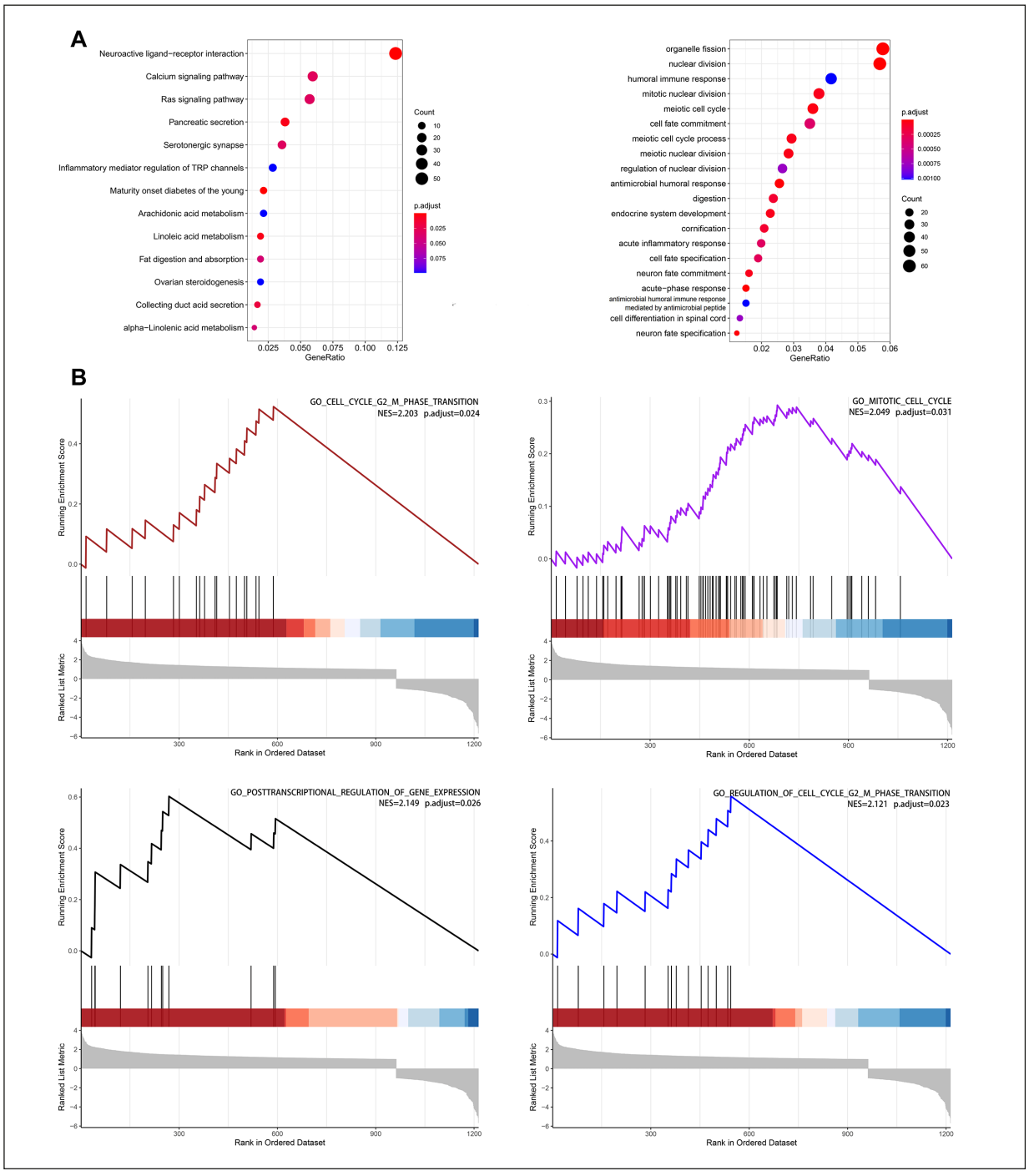

Figure 3. Functional enrichment analysis of differentially expressed genes (DEG) in KIRC samples with high and low *EME1* expression. **A**, KEGG and GO analysis of DEGs among the *EME1* expression datasets. **B**, The gene set enrichment analysis for *EME1* in clear cell renal cell carcinoma. GO items including the cell cycle G2 M phase transition, mitotic cell cycle, post-transcriptional regulation of gene expression, and the regulation of cell cycle G2 M phase transition indicated a significant differential enrichment in the *EME1* high expression phenotype.

mote the expression of immune checkpoints in clear cell renal cell carcinoma, thereby promoting the immune escape of cancer cells, resulting in poor prognosis in KIRC patients.

The Analytical Value of EME1 Pan-Cancer

To investigate whether there is a broad value for *EME1* expression, we further analyzed the *EME1* expression in a wide range of cancers. The

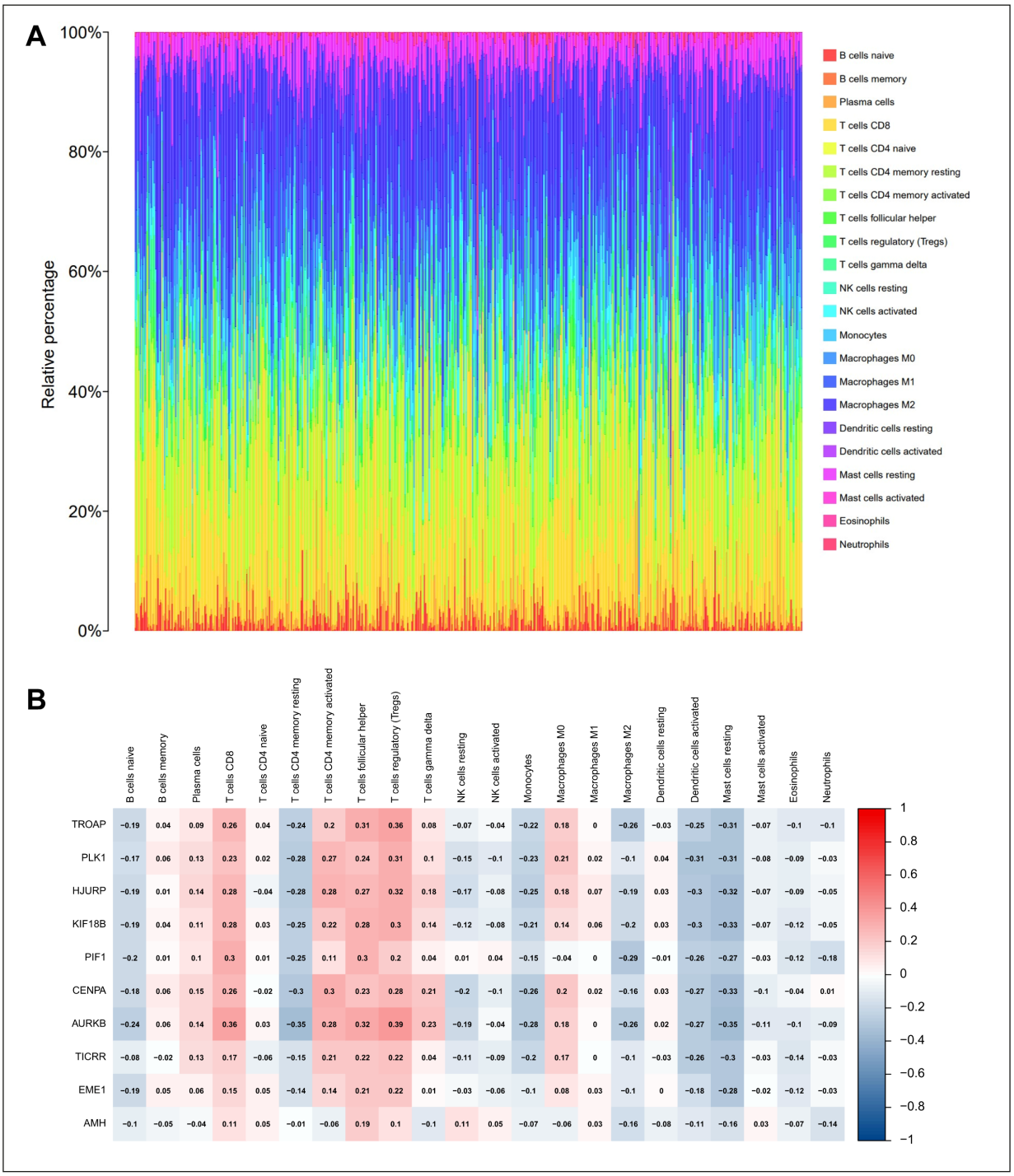

Figure 4. Levels of associated immune infiltrating cells in KIRC. **A**, Barplot indicating the distribution of 22 immune cells in clear cell renal cell carcinoma. **B**, The correlation Heatmap depicting 22 immune cells of 10 genes in clear cell renal cell carcinoma. (*EME1* was significantly correlated with CD8+ T cells, follicular helper T cells, Tregs, and mast cells).

expression of *EME1* in different cancers is depicted in the Gene Expression Profiling Interactive Analysis (GEPIA) (Figure 6A). The analysis of TISIDB results suggested that the high expression of *EME1* pan-cancer tended to be associated with shorter OS of the tumor (Figure 6B), advanced tumor stage (Figure 6C), and higher tumor grade (Figure 6D). Among them, clear cell

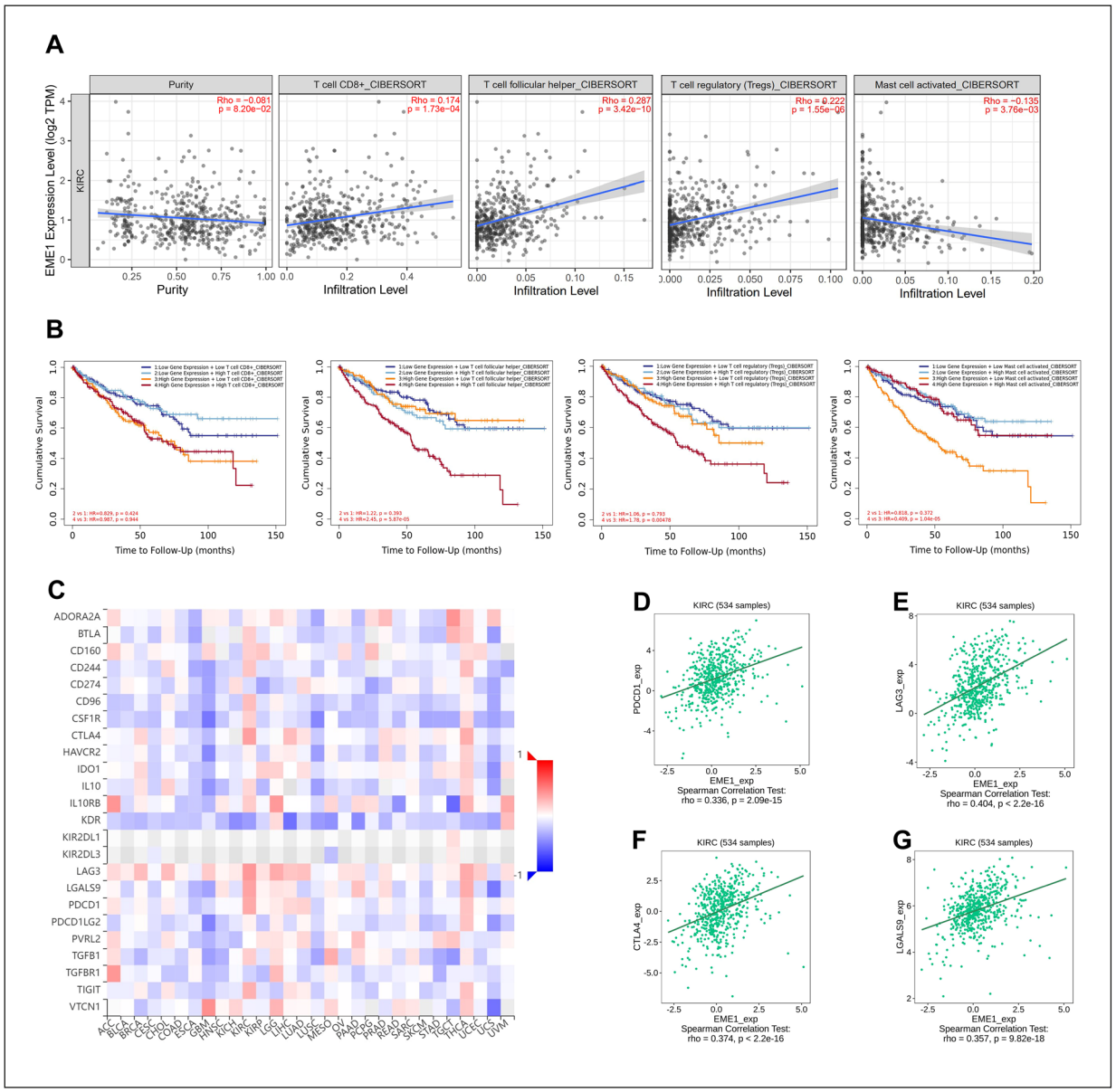

Figure 5. Potential effects of *EME1* on immune cell infiltration of clear cell renal cell carcinoma. **A**, Correlation of the *EME1* expression with immune infiltration levels in clear cell renal cell carcinoma. (The *EME1* expression was positively correlated with the infiltration level of CD8+ T cells (r = 0.174, *p* = 1.73e-04), follicular helper T cells (r = 0.287, *p* = 3.24e-10), and Tregs (r = 0.222, *p* = 1.55e-06) and negatively correlated with the infiltration level of mast cells (r = -0.135, *p* = 3.76e-03). **B**, The cumulative survival rate of clear cell renal cell carcinoma is related to follicular helper T cells, Tregs, and mast cells (mast cell infiltration is associated with better cumulative survival). **C**, Relationship between the *EME1* expression and different immune checkpoints based on the TISIDB database. **D**, *PDCD1*. **E**, *LAG3*. **F**, *CTLA4*. **G**, *LGALS9*.

renal cell carcinoma was more prominent (Figures 6E and F). This finding is consistent with the results of the above-mentioned study. According to Kaplan-Meier survival analysis, the telltale expression of *EME1* was associated with adrenocortical carcinoma (ACC), kidney renal clear cell carcinoma (KIRC), kidney renal papillary cell carcinoma (KIRP), brain Lower Grade Glioma (LGG), liver hepatocellular carcinoma (LIHC), lung adenocarcinoma (LUAD), mesothelioma (MESO), pancreatic adenocarcinoma (PAAD), skin cutaneous melanoma (SKCM), and uterine corpus endometrial carcinoma (UCEC) was associated with low survival rates (Figures 6G-P).

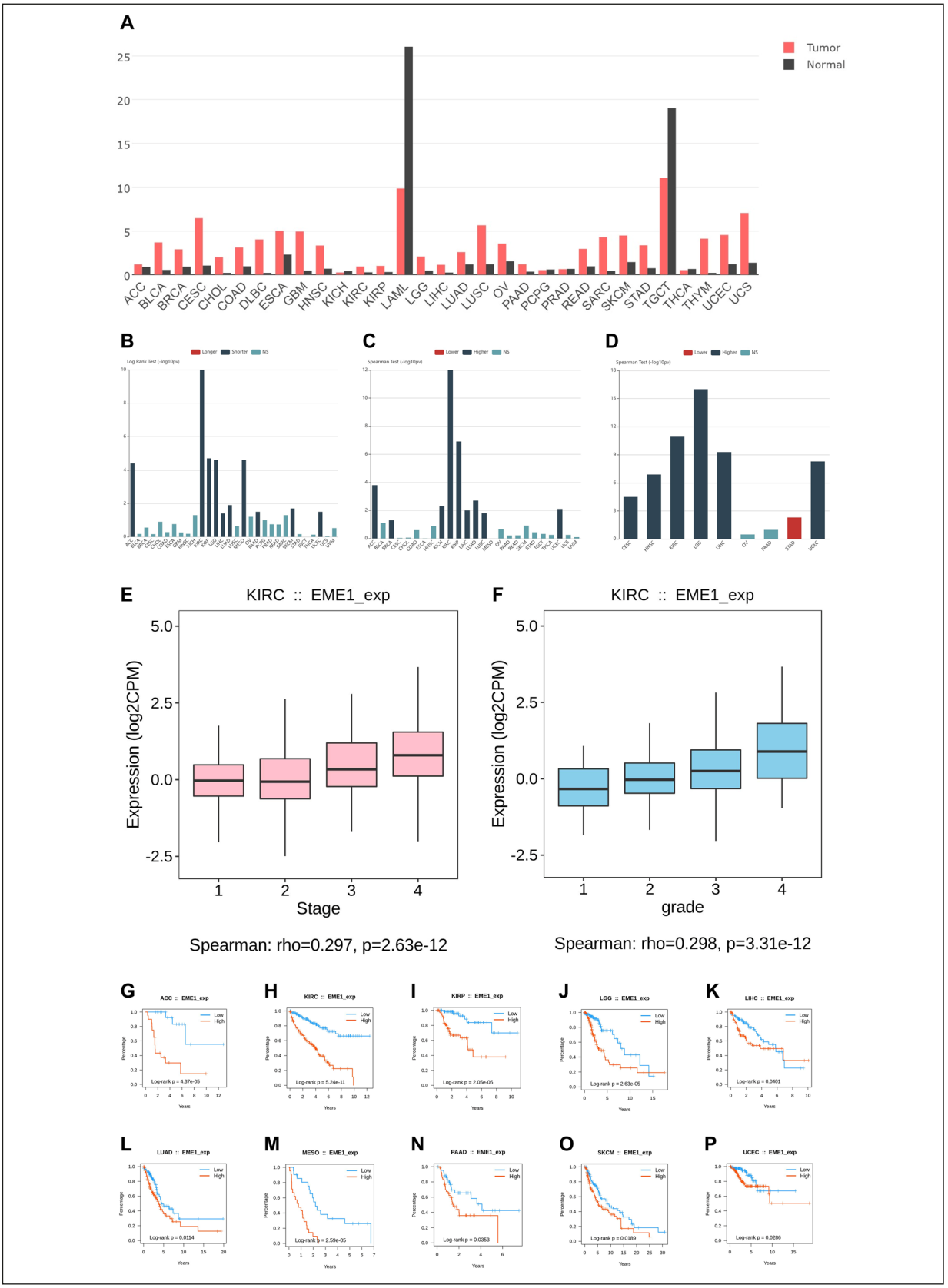

Figure 6. Expression of *EME1* in pan-cancerous tissues and the value. **A**, Comparison of the difference in the *EME1* expression between pan-cancerous and normal tissues based on the GEPIA database. **B**, Relationship between the *EME1* expression and overall survival in human cancers based on the TISIDB database. **C**, Relationship between the *EME1* expression and human cancer stage based on the TISIDB database. **D**, Relationship between *EME1* expression and human cancer grade based on the TISIDB database. **E**, Relationship between the *EME1* expression and clear cell renal cell carcinoma stage based on the TISIDB database. **F**, Relationship between the *EME1* expression and clear cell renal cell carcinoma grade based on the TISIDB database. **G**, Kaplan-Meier deep valley adoption-survival analysis between the high and low *EME1* expression groups based on the TISIDB database (**G**) ACC, (**H**) KIRC, (**I**) KIRP, (**J**) LGG, (**K**) LIHC, (**L**) LUAD, (**M**) MESO, (**N**) PAAD, (**O**) SKCM, and (**P**) UCEC.

Exploring EME1 Expression in KIRC for Positively and Negatively Correlated Gene Clusters

We demonstrated that the gene clusters were highly associated with the *EME1* expression in KIRC by volcano plot based on the LinkedOmics database analysis (Figure 7A). The heat map identified the top 50 genes that were positively and negatively correlated with the *EME1* expression in KIRC (Figures 7B and C).

Using Pearson's correlational analysis, we found that, in KIRC, the *EME1* expression had a strong positive correlation with *RAD54L* (r = 0.7725, $p = 8.076 \times 10^{-107}$), *CDCA3* (r = 0.772, $p = 1.417 \times 10^{-106}$), *KIF18B* (r = 0.7587, $p = 6.612 \times 10^{-101}$), *HJURP* (r = 0.7586, $p = 7.321 \times 10^{-101}$), and *TROAP* (r = 0.7577, $p = 1.75 \times 10^{-100}$) (Figure 8). We further analyzed by using GEPIA and found that *RAD54L* significantly affected the OS of KIRC patients, while *CDCA3*, *KIF18B*, *HJURP*, and *TROAP* significantly affected the OS and DFS of KIRC patients. A high expression of these genes was associated with low survival rates in KIRC patients (Figures 8A-E).

In addition, there was a strong negative correlation with *NR3C2* (r = -0.615, $p = 6.654 \times 10^{-57}$), *ITGA6* (r = -0.5908, $p = 1.811 \times 10^{-51}$), CDS1 (r = -0.5667, $p = 1.317 \times 10^{-46}$), *OSBPL1A* (r = -0.5606,

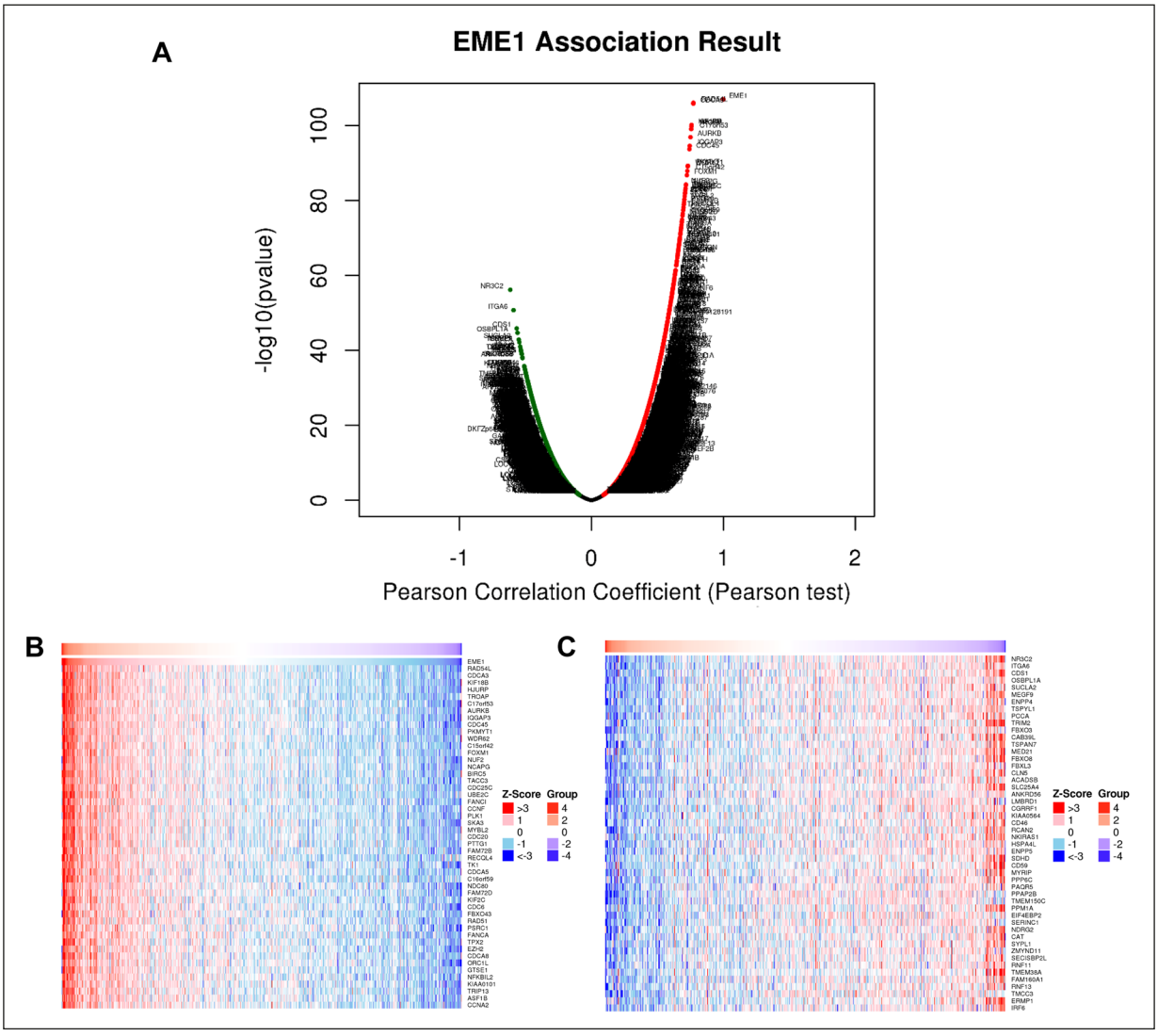

Figure 7. Analysis of genes positively and negatively associated with *EME1* in KIRC based on the LinkedOmics database. **A**, A volcano plot depicting some genes associated with the *EME1* expression in KIRC. **B**, Heat map indicating the top 50 genes that were positively associated with the *EME1* expression in KIRC. **C**, Heat map indicating the top 50 genes negatively associated with the *EME1* expression in KIRC.

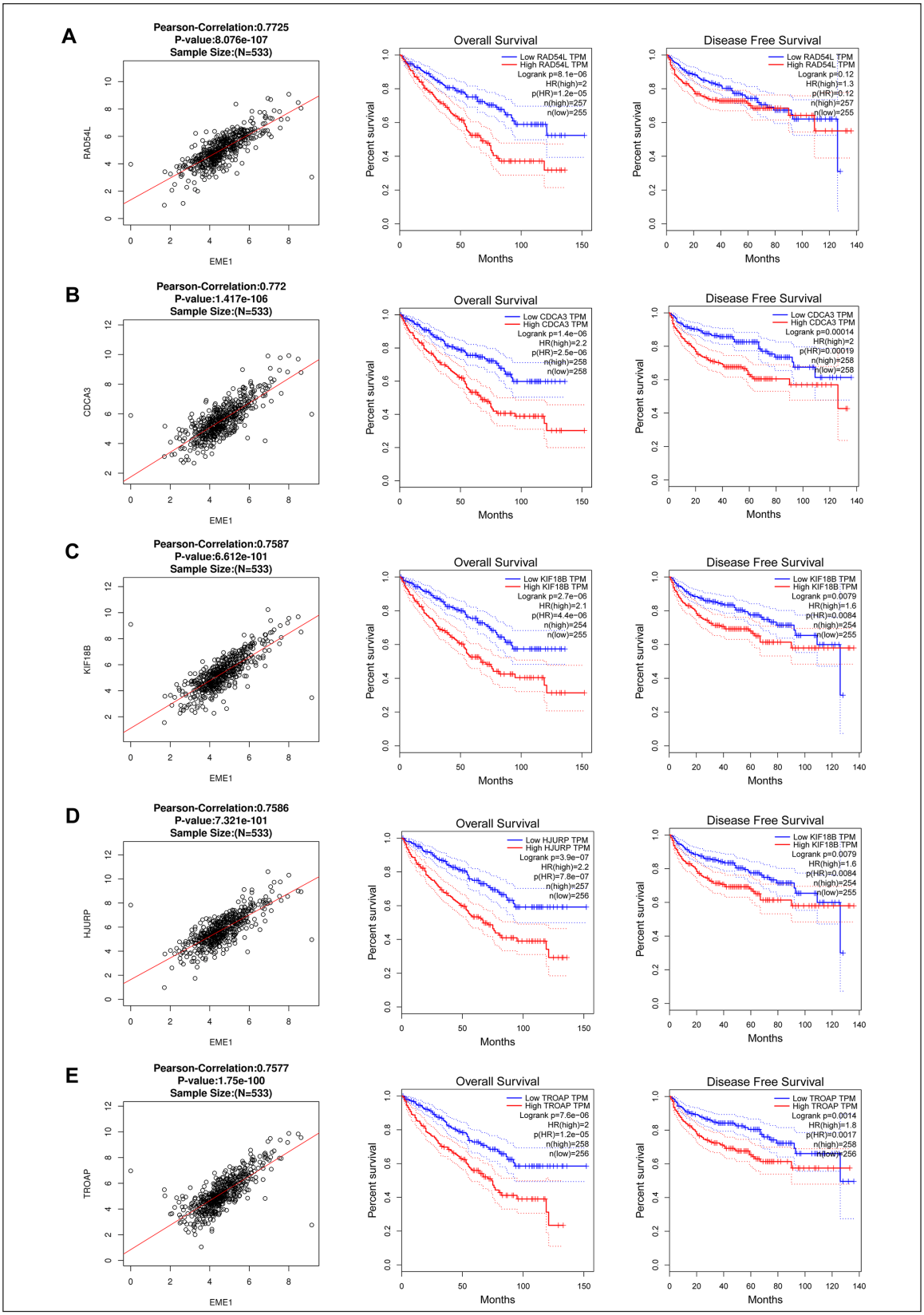

Figure 8. Based on the LinkedOmics and GEPIA databases, we analyzed the top 5 genes positively associated with the *EME1* expression in KIRC and their prognosis. **A**, *RAD54L*. **B**, *CDCA3*. **C**, *KIF18B*. **D**, *HJURP*. **E**, *TROAP*.

$p = 1.979 \times 10^{-45}$), and *SUCLA2* (r = -0.5508, $p = 1.289 \times 10^{-49}$) (Figure 9). These 5 genes significantly affected the OS and DFS of KIRC patients and their high expression was associated with better survival rates in KIRC patients (Figures 9A-E). Overall, the five genes were significantly positively correlated with *EME1* as well as with low survival rates in KIRC patients, indicating a promoting role in cancer. The high expression of these five genes significantly negatively correlated with *EME1* was found to be associated with a high survival rate in KICR patients; hence, they may have inhibitory effects on cancer development. There related genes are further analyzed in the Discussion section. Nevertheless, these results suggest the cancer-promoting role played by *EME1* in KIRC.

Discussion

Renal cell carcinoma has several histological subtypes, of which the most common (>80%) is ccRCC[17]. Conventionally, ccRCC has been treated with sunitinib, a vascular endothelial growth factor receptor (VEGFR) tyrosine kinase inhibitor (TKI), but several patients began to subsequently develop resistance to sunitinib within a few years of treatment[18]. In addition, the incidence of ccRCC is increasing, which has seriously endangered the health of patients and imposed a serious economic burden on society.

Under normal physiological conditions, an important function of *MUS81-EME1* in common fragile sites (CFSs) is to promote DNA repair synthesis that occurs during the mitotic prophase[19]. The present study revealed that *EME1* increases together with *GEN1* (another structure-specific endonuclease) and cleared the reversed-fork Holliday junctions to promote DNA replication in cancer cells, which may be related to the proliferation of cancer cells[20,21]. *EME1* was found to be highly expressed in breast, gastric, and esophageal cancers with poor prognosis, indicating a potential mechanism to promote tumor development. For example, past studies reported that *EME1* activates the *Akt/GSK3B/CCND1* pathway to enhance GC invasiveness, leading to poor prognosis in GC patients[14]. However, the mechanism of *EME1* in ccRCC has not been elaborated, and there is a lack of relevant research literature on this subject.

Therefore, we conducted a study on the potential role of *EME1* in ccRCC. We screened the clinical data from the TCGA database of ccRCC tissues *vs.* normal tissues as well as the RNA-Seq data for a series of analyses. Our results revealed that the expression of *EME1* was significantly higher in ccRCC tissues than in normal tissues, indicating a potential relationship between *EME1* and the development of ccRCC. We also analyzed the relationship between the expression of *EME1* and the tumor stage of ccRCC and found that the expression of *EME1* was significantly higher at stage 3/4. Thus, the high expression of *EME1* is possibly related to the late progression of ccRCC. In addition, we found that the high expression of *EME1* was associated with a poor clinical prognosis of ccRCC, which was significantly associated with the advanced TNM stage. Moreover, based on the clinical prediction of the survival time for ccRCC patients, we established a nomogram model combining the high and low expression of *EME1* to determine the survival rate of patients at 1, 2, and 3 years based on the relevant clinical information of patients. The c-index of our resulting prediction model was 0.796.

It has been reported that *EME1* has a DNA repair capacity and that a low DNA repair capacity may increase the overall risk of breast cancer, while a contradictory high DNA repair capacity allows the repair of DNA damage caused by chemotherapy, which results in the development of drug resistance[22]. The increased expression of *EME1* has been associated with poor prognosis in GC, esophageal cancer, and bladder cancer. Considering these possibilities, we analyzed the predictive ability of *EME1* in ccRCC for patient prognosis based on the expression of *EME1* in tumor tissues combined with the survival time of patients, whereby we concluded that the AUC results were all >0.60, implying that *EME1* has a good ability to predict the survival of ccRCC patients. We also recorded that the likelihood of survival was substantially lower in the *EME1* high-expression group compared to that in the low-expression group, suggesting that *EME1* is an independent predictor of prognosis in ccRCC patients.

However, the role of *EME1* in ccRCC remains unclear. To further investigate the function of *EME1* in the progression of ccRCC, we performed KEGG, GO, and GSEA analysis by using the TGCA data. Based on the results of GO and GSEA enrichment analyses, we found that the high *EME1* expression is possibly associated with cell cycle regulation, meiosis, mitosis, post-transcriptional regulation of gene expression, and hu-

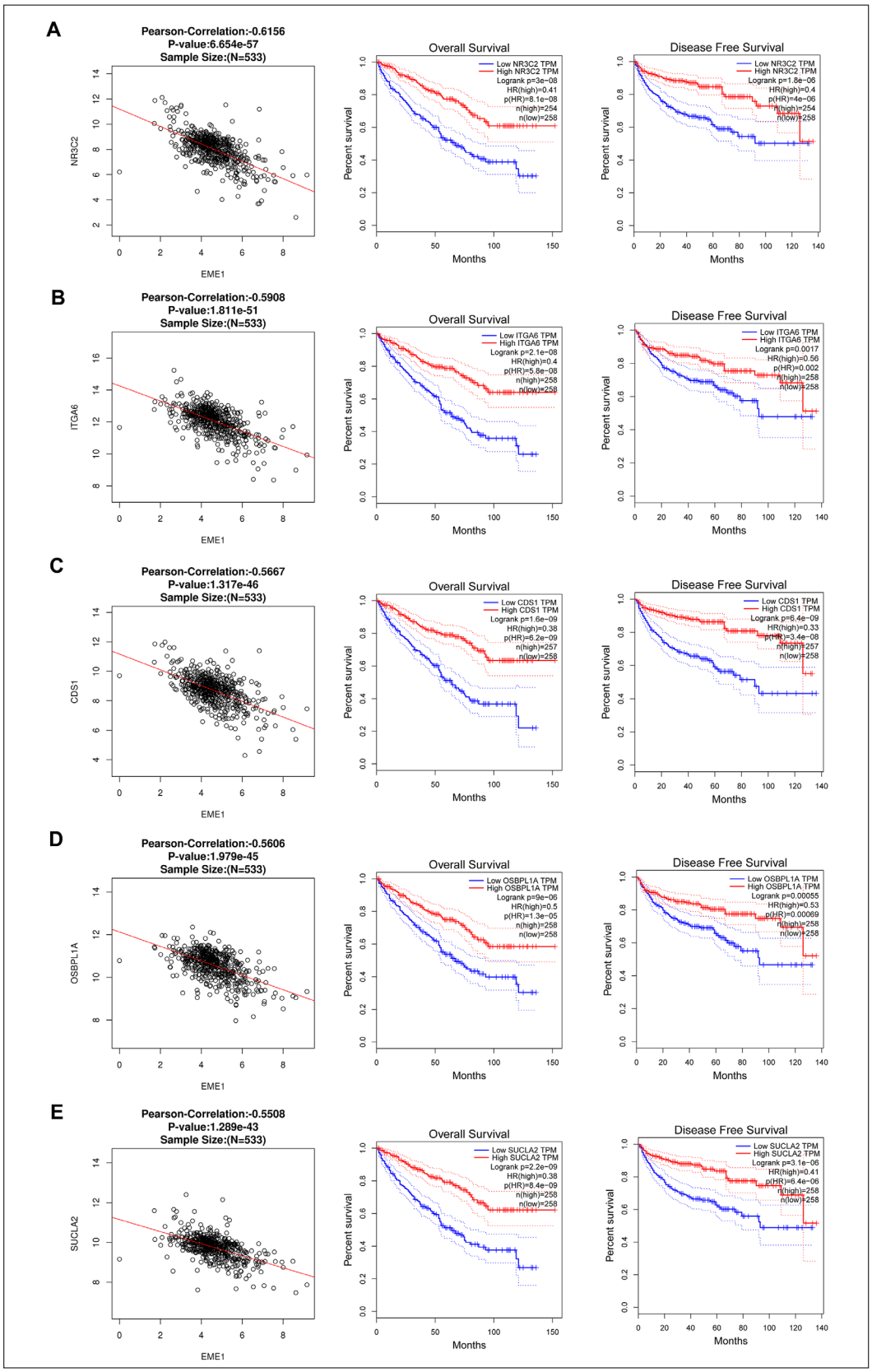

Figure 9. Based on LinkedOmics and GEPIA databases, we analyzed the top 5 genes negatively associated with the *EME1* expression in KIRC and their prognosis. **A**, *NR3C2*. **B**, *ITGA6*. **C**, *CDS1*. **D**, *OSBPL1A*. **E**, *SUCLA2*.

moral immune response. These biological functions may be important for the proliferation of ccRCC tumor cells. This evidence cumulatively suggests the potential role of *EME1* in ccRCC progression as well as that *EME1* may be a potential prognostic marker and a therapeutic target for ccRCC.

Based on several recent studies, a tumor tissue is a complex environment mainly composed of cells and showing stroma and immune cell infiltration, wherein the immune-infiltrating cells possess tumor-promoting or tumor-suppressing effects[23]. Specifically, Tregs and tumor-associated macrophages (TAMs) have the ability to promote tumorigenesis-related development[24,25]. Mast cells may promote neovascularization by releasing angiogenic factors and promote tumor aggressiveness by releasing matrix metalloprotein matrix metalloproteinases (MMP)[26,27]. In contrast, another study[28] reported that mast cells play a unique anti-tumor function in nasopharyngeal carcinoma, suggesting a dual role for mast cells in influencing the development of different tumors. Follicular helper T cells play an important role in the formation and maintenance of germinal centers (GCs) and can help B cells produce an effective antibody response, thereby allowing a better prognostic outcome that is associated with the presence of some solid tumors[29,30]. Tregs are a highly immunosuppressive cell population, which helps maintain immune homeostasis and prevent the occurrence of autoimmune diseases. However, they also inhibit the body's immune surveillance of tumors and prevent the host from generating an effective anti-tumor immune response, thereby promoting the development and progression of tumors[31]. Thus, a high degree of infiltration of Tregs in tumors has been associated with low survival in various cancers[32]. Some scholars[33] have reported that the occurrence and development of ccRCC are closely related to its immune microenvironment and that the TME has a significant relationship with the development of tumors. It is therefore evident that this aspect of tumor immune cell infiltration has become a hot topic for research recently; therefore, the correlation between *EME1* in ccRCC and immune cell infiltration has been further analyzed. An analysis of the Cibersort and TIMER online database revealed that the expression of *EME1* in ccRCC was significantly and positively correlated with the infiltration level of follicular helper T cells and Tregs and negatively correlated with the infiltration level of Mast cells. Interestingly, we found that mast cell infiltration was associated with better cumulative survival in ccRCC, whereas the *EME1* expression was correlated with mast cells. Therefore, the effect of *EME1* on ccRCC may be associated with the infiltration of Tregs and the reduction of mast cells. We further analyzed *EME1* with reference to the GEPIA and TISIDB databases and found that a high *EME1* expression was associated with poor prognosis in most tumors, which is consistent with our previous findings. We further analyzed that a high *EME1* expression in ccRCC was associated with immune cell surface receptors, mainly PDCD1, LAG3, CTLA4, and LGALS9. These immune checkpoints have been extensively studied for their role in tumor immune escape in a wide range of tumors as well as for their widespread applications as therapeutic targets[34]. This finding suggested that the high expression of *EME1* in ccRCC may be associated with some inhibitory immune cell surface receptors. Accordingly, the specific mechanism of *EME1* involvement in ccRCC immune infiltration warrants further investigation to provide new ideas for subsequent immunotherapy.

Based on Pearson's correlational analysis from the LinkedOmics database, we noted a positive correlation between the *EME1* expression and *RAD54L*, *CDCA3*, and *KIF18B* in ccRCC. Previous studies[35,36] reported that *RAD54L* may be involved in DNA recombination as well as DNA repair, which is associated with breast carcinogenesis as well as radiation therapy resistance in head and neck squamous cell carcinoma. *CDCA3* regulates the cell cycle and is often upregulated in tumor tissues, while the knockdown of *CDCA3* can regulate the NF-κB signaling pathway to inhibit cell cycle protein D1 expression so as to suppress prostate cancer progression[37]. In fact, *KIF18B* was found to be highly expressed in breast cancer tissues and involved in the promotion of proliferation, migration, and invasion of breast cancer cells[38]. On the other hand, a strong negative correlation was noted between the *EME1* expression and *NR3C2* in ccRCC. *NR3C2* was found to be under-expressed in the colon and renal cell carcinoma tissues. The overexpression of *NR3C2* could inhibit tumor cell proliferation, migration, invasion, and angiogenesis in colon and renal cell carcinomas[39,40]. *CDS1* was found to be poorly expressed in hepatocellular carcinoma cells as a result of methylation of this gene[41]. For the five genes positively associated with *EME1*,

we analyzed that their high expression was associated with a low KIRC survival. Interestingly, for the 5 genes negatively associated with *EME1*, their high expression was associated with a good prognosis of KIRC. Thus, the role of *EME1* in KIRC as a cancer-promoting agent is ascertained. Based on the bioinformatics analysis combined with the results of previous studies, the expression of *EME1* in different tumors is likely to indicate the promotion of tumor development and poor prognosis.

Conclusions

In conclusion, overexpression of *EME1* in the ccRCC tissues was observed, which indicated that a high expression of *EME1* correlates with poor prognosis in ccRCC. In addition, the critical biological functions regulated by *EME1* in ccRCC may be related to cell cycle regulation, cell division, and humoral immunity. Finally, further findings suggested that *EME1* may be involved in ccRCC-related immune infiltration to influence tumor progression. In this regard, further research is warranted in this field to continuously refine our understanding of the biological impact of *EME1*.

This research results show that overexpression of EME1 is associated with poor prognosis in renal clear cell carcinoma. Meanwhile, there is a correlation between EME1 and immune infiltration. It suggests that EME1 may be a potential therapeutic target for renal clear cell carcinoma.

Conflict of Interest

The authors declare that they have no conflict of interests.

Acknowledgements

We thank Nurse Lee for her help in collecting data for us.

Ethics Approval

Not applicable.

Informed Consent

All the data were collected and downloaded from TCGA and GEO database. As TCGA and GEO database are open to the public under specific guidelines, it is confirmed that all written-informed consents were achieved.

ORCID iD

Haodong Li: 0009-0003-7216-9550
Jianguo Ma: 0009-0005-6908-1747

Authors' Contribution

Authors Haodong, Li and Hongxuan, Ma contributed equally to this paper, including conceptualizing the concept, data collection, analyzing the data, and writing the paper. The other authors played a coordinating role in the above.

Funding

This study was supported by the Hebei Provincial Excellent Talents in Clinical Medicine
Project (2022180).

Data Availability

The data used in this study (TCGA) can be downloaded from the UCSC Xena network (https://xenabrowser.net/datapages/). GEO database (https://www.ncbi.nlm.nih.gov/geo/), including GSE40435, GSE53000, GSE68417, and GSE53757. All the above datasets are open access datasets.

References

1) Siegel RL, Miller KD, Fuchs HE, Jemal A. Cancer Statistics, 2021. CA Cancer J Clin 2021; 71: 7-33.
2) Jonasch E, Gao J, Rathmell WK. Renal cell carcinoma. BMJ 2014; 349: g4797.
3) Choueiri TK, Motzer RJ. Systemic Therapy for Metastatic Renal-Cell Carcinoma. N Engl J Med 2017; 376: 354-366.
4) Jian Y, Yang K, Sun X, Zhao J, Huang K, Aldanakh A, Xu Z, Wu H, Xu Q, Zhang L, Xu C, Yang D, Wang S. Current Advance of Immune Evasion Mechanisms and Emerging Immunotherapies in Renal Cell Carcinoma. Front Immunol 2021; 12: 639636.
5) Díaz-Montero CM, Rini BI, Finke JH. The immunology of renal cell carcinoma. Nat Rev Nephrol 2020; 16: 721-735.
6) Boddy MN, Gaillard PHL, McDonald WH, Shanahan P, Yates JR, 3rd, Russell P. Mus81-Eme1 are essential components of a Holliday junction resolvase. Cell 2001; 107: 537-548.
7) Abraham J, Lemmers B, Hande MP, Moynahan ME, Chahwan C, Ciccia A, Essers J, Hanada K, Chahwan R, Khaw AK, McPherson P, Shehabeldin A, Laister R, Arrowsmith C, Kanaar R, West SC, Jasin M, Hakem R. Eme1 is involved in DNA damage processing and maintenance of genomic stability in mammalian cells. Embo j 2003; 22: 6137-6147.
8) Calzetta NL, González Besteiro MA, Gottifredi V. Mus81-Eme1-dependent aberrant processing of DNA replication intermediates in mitosis impairs genome integrity. Sci Adv 2020; 6: eabc8257.

9) Vigneron A, Gamelin E, Coqueret O. The EGFR-STAT3 oncogenic pathway up-regulates the Eme1 endonuclease to reduce DNA damage after topoisomerase I inhibition. Cancer Res 2008; 68: 815-825.

10) Tomoda Y, Katsura M, Okajima M, Hosoya N, Kohno N, Miyagawa K. Functional evidence for Eme1 as a marker of cisplatin resistance. Int J Cancer 2009; 124: 2997-3001.

11) Weinandy A, Piroth MD, Goswami A, Nolte K, Sellhaus B, Gerardo-Nava J, Eble M, Weinandy S, Cornelissen C, Clusmann H, Lüscher B, Weis J. Cetuximab induces eme1-mediated DNA repair: a novel mechanism for cetuximab resistance. Neoplasia 2014; 16: 207-220, 220.e201-204.

12) Carter R, Westhorpe A, Romero MJ, Habtemariam A, Gallevo CR, Bark Y, Menezes N, Sadler PJ, Sharma RA. Radiosensitisation of human colorectal cancer cells by ruthenium(II) arene anticancer complexes. Sci Rep 2016; 6: 20596.

13) Han Y, Zheng Q, Tian Y, Ji Z, Ye H. Identification of a nine-gene panel as a prognostic indicator for recurrence with muscle-invasive bladder cancer. J Surg Oncol 2019; 119: 1145-1154.

14) Guo Z, Liang E, Li W, Jiang L, Zhi F. Essential meiotic structure-specific endonuclease1 (EME1) promotes malignant features in gastric cancer cells via the Akt/GSK3B/CCND1 pathway. Bioengineered 2021; 12: 9869-9884.

15) Zhao J, Liu L, Zhang A, Chen Q, Fang W, Zeng L, Lu J. Effect of EME1 exon variant Ile350Thr on risk and early onset of breast cancer in southern Chinese women. J Biomed Res 2013; 27: 193-201.

16) MacGregor TP, Carter R, Gillies RS, Findlay JM, Kartsonaki C, Castro-Giner F, Sahgal N, Wang LM, Chetty R, Maynard ND, Cazier JB, Buffa F, McHugh PJ, Tomlinson I, Middleton MR, Sharma RA. Translational study identifies XPF and MUS81 as predictive biomarkers for oxaliplatin-based peri-operative chemotherapy in patients with esophageal adenocarcinoma. Sci Rep 2018; 8: 7265.

17) Choueiri TK, Kaelin WG, Jr. Targeting the HIF2-VEGF axis in renal cell carcinoma. Nat Med 2020; 26: 1519-1530.

18) Hu J, Chen Z, Bao L, Zhou L, Hou Y, Liu L, Xiong M, Zhang Y, Wang B, Tao Z, Chen K. Single-Cell Transcriptome Analysis Reveals Intratumoral Heterogeneity in ccRCC, which Results in Different Clinical Outcomes. Mol Ther 2020; 28: 1658-1672.

19) Minocherhomji S, Ying S, Bjerregaard VA, Bursomanno S, Aleliunaite A, Wu W, Mankouri HW, Shen H, Liu Y, Hickson ID. Replication stress activates DNA repair synthesis in mitosis. Nature 2015; 528: 286-290.

20) Xia J, Mei Q, Rosenberg SM. Tools To Live By: Bacterial DNA Structures Illuminate Cancer. Trends Genet 2019; 35: 383-395.

21) Minocherhomji S, Hickson ID. Structure-specific endonucleases: guardians of fragile site stability. Trends Cell Biol 2014; 24: 321-327.

22) Matta J, Morales L, Dutil J, Bayona M, Alvarez C, Suarez E. Differential expression of DNA repair genes in Hispanic women with breast cancer. Mol Cancer Biol 2013; 1: 54.

23) Şenbabaoğlu Y, Gejman RS, Winer AG, Liu M, Van Allen EM, de Velasco G, Miao D, Ostrovnaya I, Drill E, Luna A, Weinhold N, Lee W, Manley BJ, Khalil DN, Kaffenberger SD, Chen Y, Danilova L, Voss MH, Coleman JA, Russo P, Reuter VE, Chan TA, Cheng EH, Scheinberg DA, Li MO, Choueiri TK, Hsieh JJ, Sander C, Hakimi AA. Tumor immune microenvironment characterization in clear cell renal cell carcinoma identifies prognostic and immunotherapeutically relevant messenger RNA signatures. Genome Biol 2016; 17: 231.

24) Nishikawa H, Sakaguchi S. Regulatory T cells in cancer immunotherapy. Curr Opin Immunol 2014; 27: 1-7.

25) Noy R, Pollard JW. Tumor-associated macrophages: from mechanisms to therapy. Immunity 2014; 41: 49-61.

26) Komi DEA, Redegeld FA. Role of Mast Cells in Shaping the Tumor Microenvironment. Clin Rev Allergy Immunol 2020; 58: 313-325.

27) Paolino G, Corsetti P, Moliterni E, Corsetti S, Didona D, Albanesi M, Mattozzi C, Lido P, Calvieri S. Mast cells and cancer. G Ital Dermatol Venereol 2019; 154: 650-668.

28) Cheng S, Li Z, Gao R, Xing B, Gao Y, Yang Y, Qin S, Zhang L, Ouyang H, Du P, Jiang L, Zhang B, Yang Y, Wang X, Ren X, Bei JX, Hu X, Bu Z, Ji J, Zhang Z. A pan-cancer single-cell transcriptional atlas of tumor infiltrating myeloid cells. Cell 2021; 184: 792-809.e723.

29) Mintz MA, Cyster JG. T follicular helper cells in germinal center B cell selection and lymphomagenesis. Immunol Rev 2020; 296: 48-61.

30) Baumjohann D, Brossart P. T follicular helper cells: linking cancer immunotherapy and immune-related adverse events. J Immunother Cancer 2021; 9: eabc8257.

31) Togashi Y, Shitara K, Nishikawa H. Regulatory T cells in cancer immunosuppression - implications for anticancer therapy. Nat Rev Clin Oncol 2019; 16: 356-371.

32) Ohue Y, Nishikawa H. Regulatory T (Treg) cells in cancer: Can Treg cells be a new therapeutic target? Cancer Sci 2019; 110: 2080-2089.

33) Wang Y, Yin C, Geng L, Cai W. Immune Infiltration Landscape in Clear Cell Renal Cell Carcinoma Implications. Front Oncol 2020; 10: 491621.

34) Sasidharan Nair V, Toor SM, Taha RZ, Shaath H, Elkord E. DNA methylation and repressive histones in the promoters of PD-1, CTLA-4, TIM-3, LAG-3, TIGIT, PD-L1, and galectin-9 genes in human colorectal cancer. Clin Epigenetics 2018; 10: 104.

35) Helgadottir HT, Thutkawkorapin J, Lagerstedt-Robinson K, Lindblom A. Sequencing for germline mutations in Swedish breast cancer families reveals novel breast cancer risk genes. Sci Rep 2021; 11: 14737.

36) Nathansen J, Lukiyanchuk V, Hein L, Stolte MI, Borgmann K, Löck S, Kurth I, Baumann M, Krause M, Linge A, Dubrovska A. Oct4 confers stemness and radioresistance to head and neck squamous cell carcinoma by regulating the homologous recombination factors PSMC3IP and RAD54L. Oncogene 2021; 40: 4214-4228.

37) Gu P, Zhang M, Zhu J, He X, Yang D. Suppression of CDCA3 inhibits prostate cancer progression via NF-κB/cyclin D1 signaling inactivation and p21 accumulation. Oncol Rep 2022; 47.

38) Liu L, Zhang Z, Xia X, Lei J. KIF18B promotes breast cancer cell proliferation, migration and invasion by targeting TRIP13 and activating the Wnt/β-catenin signaling pathway. Oncol Lett 2022; 23: 112.

39) Zhao Z, Zhang M, Duan X, Deng T, Qiu H, Zeng G. Low NR3C2 levels correlate with aggressive features and poor prognosis in non-distant metastatic clear-cell renal cell carcinoma. J Cell Physiol 2018; 233: 6825-6838.

40) Li J, Xu Z. NR3C2 suppresses the proliferation, migration, invasion and angiogenesis of colon cancer cells by inhibiting the AKT/ERK signaling pathway. Mol Med Rep 2022; 25: 133.

41) Yeh KT, Tang KP, Chen YL, Su WW, Wang YF, Chang JG. Methylation Inactivates Expression of CDP-diacylglycerol Synthase 1 (CDS1) in Hepatocellular Carcinoma. Cancer Genomics Proteomics 2006; 3: 231-238.